

www.acsami.org Research Article

Starch Janus Particles: Bulk Synthesis, Self-Assembly, Rheology, and Potential Food Applications

Arkaye Kierulf, Mojtaba Enayati, Mohammad Yaghoobi, Judith Whaley, James Smoot, Mariana Perez Herrera, and Alireza Abbaspourrad*



Cite This: ACS Appl. Mater. Interfaces 2022, 14, 57371–57386



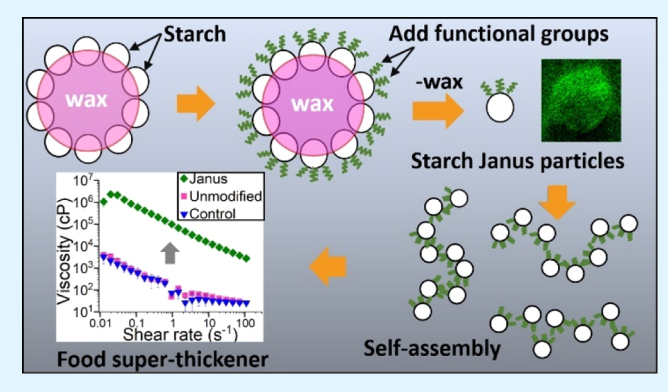
ACCESS I

III Metrics & More

Article Recommendations

s Supporting Information

ABSTRACT: Although incredible progress in the field of Janus particles over the last three decades has delivered many promising smart-material prototypes, from cancer-targeting drug delivery vehicles to self-motile nanobots, their real-world applications have been somewhat tempered by concerns over scalability and sustainability. In this study, we adapt a simple, scalable 3D mask method to synthesize Janus particles in bulk using starch as the base material: a natural biopolymer that is safe, biocompatible, biodegradable, cheap, widely available, and versatile. Using this method, starch granules are first embedded on a wax droplet such that half of the starch is covered; then, the uncovered half is treated with octenyl succinic anhydride, after which the wax coating is removed. Janus particles with 49% Janus balance can be produced



in this way and were observed to self-assemble into wormlike strings in water due to their hydrophobic/hydrophilic nature. Our Janus starch granules outperform the non-Janus controls as thickening and gelling agents: they exhibit a fourfold increase in water-holding capacity, a 30% lower critical caking concentration, and a viscosity greater by orders of magnitude. They also form gels that are much firmer and more stable. Starch Janus particles with these functional properties can be used as novel, lower-calorie, highly efficient, plant-based super-thickeners in the food industry, potentially reducing starch use in food by 55%.

KEYWORDS: Janus particles, amaranth starch, bulk synthesis, natural biopolymers, octenyl succinic anhydride, thickeners, texturizers, and gelling agents

■ INTRODUCTION

Food products worldwide rely on starch as a thickener to deliver the viscosity and texture that consumers have come to expect from their favorite foods: from soups to tomato sauce, yogurts to cakes, and from beverages to plant-based meats. The global modified food starch market is worth \$12.6 billion annually and is expected to grow 3-6% every year to catch up with this demand. For the past 50-70 years, food companies have relied on the same classic starch swelling mechanism in water to build viscosity: heat and shear make starch granules swell. These swollen starches then take up a larger effective dispersed phase volume, making them bump and jam against each other. This restricts the flow of the fluid and builds viscosity. A new mechanism to build viscosity will open the door to a new generation of starch super-thickeners that can provide new food textures, potential dual reductions in calories and food manufacturing costs, and other enhanced applications where a food-safe, biodegradable, and self-assembling material is needed.² Janus particles, particles with two opposite halves with different physical or chemical functionalities,³ have the potential of providing this new mechanism: interparticle selfassembly.

In material science, Janus particles have attracted a lot of attention due to their unique asymmetric properties, making them prime candidates for smart materials. First produced in the 1980s, then popularized in the 1990s by the Nobel Laureate de Gennes, they have now been synthesized via many different techniques using different starting materials, and intended for a wide array of applications. Janus particles are currently being developed as targeted drug delivery vehicles for cancer treatments, self-mixing micro- and nano-motors for pollution removal, surfactants, sensors/probes, electronics, and coatings.

Optimism over the early promise demonstrated by these synthetic Janus particles, however, has been tempered by two major hurdles: scalability and sustainability. First, existing methods to make Janus particles from solid or liquid starting

Received: September 29, 2022 Accepted: December 5, 2022 Published: December 19, 2022





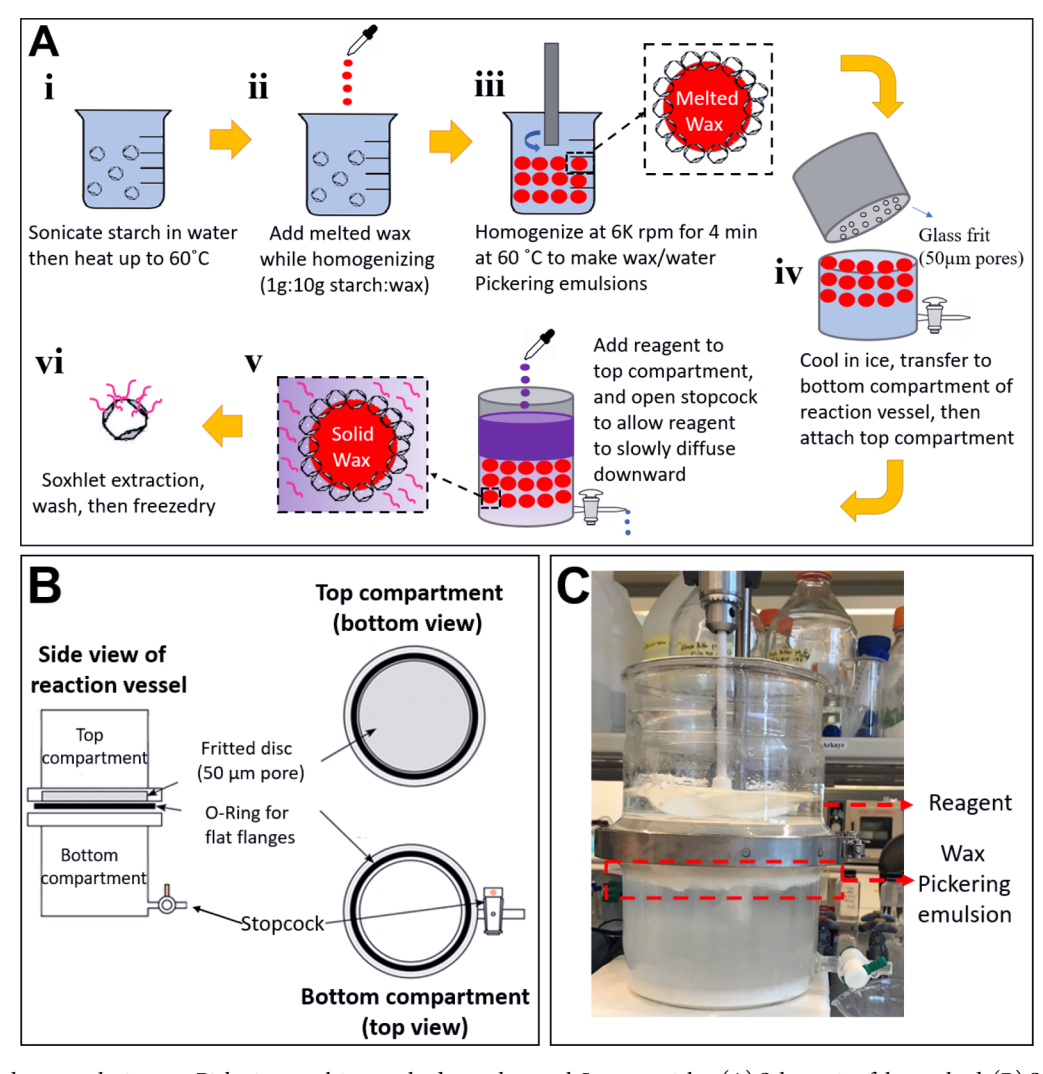


Figure 1. 3D mask approach via a wax Pickering emulsion method to make starch Janus particles. (A) Schematic of the method. (B) Schematic and (C) image of the reaction vessel used in this method (top and bottom compartments each have 1.2 L capacity). Bottom compartment holds the wax Pickering emulsion containing the starch granules to be modified and has a bottom stopcock which controls the reagent flow from the top compartment through the fritted disc to the bottom.

materials, such as the 2D mask approach, ¹⁰ phase separation, ^{11,12} and block copolymer self-assembly, ¹³ are complex, time-consuming, or have low yield, typically in the milligram scale. Second, these methods typically use toxic, expensive, nonenvironmentally friendly, nonbiocompatible, or nonbiodegradable synthetic materials that seriously hamper their potential applications in the environmental, cosmetic, biotech, and food sectors.

Perhaps the most promising strategy to resolve the first hurdle, scalability, has been the development of the 3D mask approach, with yields in the gram scale, ¹⁴ and a promising strategy to resolve the second hurdle, sustainability, has been the replacement of synthetic polymers with alternative natural biopolymers, such as alginates, chitosan, pectin, cellulose, and starch, that may be recovered, recycled, or reused. ^{3,15,16} Recent literature reports show that the second hurdle has been overcome, but the first still presents a problem. Magnetic-field-guided and uniaxial precipitation methods, for example, have been used to make Janus particles from starch that can deliver drugs to deep wounds using magnetic guidance or self-propulsion. ^{17,18} A microfluidic method has also been used to make pectin—alginate Janus microbeads for selective, controlled

release of active substances. ^{19,20} These cases however have resulted in low yields, at several micrograms or microliters per hour. Even when natural biopolymers are used, the multistep methods employed to make Janus particles are generally complex and nonscalable, thus curbing their commercial applications. ^{7,21}

We address the two main hurdles, complex synthetic methods and the unsustainable use of synthetic polymers, by first adapting a simple, scalable 3D mask method first developed by Granick et al., 14 and second by customizing and applying that method to one of the most familiar and widely used ingredients in the food industry, starch. Janus particles built on a starch platform would be considered a game changer in the food industry, offering a new generation of super-thickeners that employ a new mechanism for building viscosity based on interparticle self-assembly. In our previous work, we have already demonstrated that starch-based Janus particles made by a 2D mask approach self-assemble into wormlike strings in water, which we hypothesized could lead to super-thickening abilities.²¹ There is strong evidence to support this because our lab has recently demonstrated that patchy particles, a close cousin to Janus particles, can self-assemble and provide an

improvement in viscosity up to three orders of magnitude higher than controls. ^{22,23} This self-assembly mechanism, alone or in tandem with the classic swelling mechanism, could revolutionize the starch market by allowing the food industry to use less added starch, naturally reducing the caloric content of food products for the consumer while also lowering manufacturing cost-in-use for the food manufacturer. In addition, these new starch-based Janus particles provide potential for new textures in foods and by extension new food products that can give consumers new mouthfeel experiences, and because starch is a cheap, versatile material whose porosity, swelling, and chemical properties can be easily fine-tuned, they also have potential applications in other fields like drug delivery.

Therefore, as proof of concept, we have (1) produced Janus particles in bulk using a simple, scalable, 3D mask method; (2) used a versatile, cheap, natural biopolymer like starch granules to make these Janus particles; and (3) demonstrated that these starch Janus particles self-assemble and provide greater thickening and gelling properties than traditional, non-Janus starch. Ultimately, the importance of this work stems from the potential use of these starch Janus particles in the food industry as super-thickeners.

MATERIALS AND METHODS

Materials. Amaranth starch was extracted from a commercially available flour. Low-melting-point paraffin wax (IGI 4630 Harmony Blend Wax, MP 48 °C) was purchased from Candle Science (Durham, NC, USA). Sodium hydroxide (NaOH, 95-100%) beads were purchased from Fisher Scientific (NJ, USA). ACS-grade hydrochloric acid (HCl, 36.5-38%) was purchased from VWR Chemicals (PA, USA). n-Octenyl succinic anhydride (OSA) was provided by Dixie Chemical Company (Pasadena, Texas, USA). High-purity glass microfiber extraction thimbles (30 \times 100 mm, 0.8 μ m particle retention) were purchased from GE Life Sciences (PA, USA). ACSgrade chloroform was purchased from Midland Scientific Inc. (NE, USA). 3-Acrylamidopropyl trimethylammonium chloride (APTMAC) aqueous solution (75 w/w %, Santa Cruz Biotechnology), tris[2-(dimethylamino)ethyl]amine (Me6-TREN, Sigma-Aldrich), copper nanopowder (25 nm, Sigma-Aldrich), 2-bromopropionyl bromide (97%, Alfa Aesar), acetone (99.8% Certified ACS, Fisher), NEt3 (99.91%, Chem-Impex), and acetonitrile (99.5+% EMD Chemicals Inc.) were all used as received. Chloroform-d (99.8%) and deuterium oxide (99.9%) were purchased from Cambridge Isotope Laboratories, Inc. (MA, USA), and acetone- d_6 (99.9%) was purchased from Aldrich (MO, USA).

Isolation of Amaranth Starch from Flour. High-protein amaranth starch was isolated from a commercially available flour using an alkaline method as previously reported.²⁴ Briefly, 2 L of 0.15 w/v % NaOH was added to 400 g flour and then stirred for 1 h at 500 rpm using an overhead stirrer at room temperature. The slurry was filtered through a 270-mesh sieve (53 μ m pore size) using a laboratory test sieve vibrator (Houghton Manufacturing Co., MI, USA) for 10 min. The unfiltered residue was collected, re-dispersed in 400 mL of 0.15 w/v % NaOH, stirred for 10 min, then filtered again through the 270-mesh sieve, and washed with 200 mL of 0.15 w/v % NaOH. The filtrates were combined, then centrifuged for 20 min at 3000g. After discarding the supernatant, the top yellow-brown layer of the pellet was removed using a spatula. The white pellet was then reconstituted in water, adjusted to pH 6.0 ± 0.1 using 1 N HCl, and re-centrifuged, again removing the supernatant and the pellet's top yellow-brown layer. The isolated starch was then freeze-dried for 24 h and ground using an ultrafine conical burr grinder. The yield was approximately 12.5%, or 50 g of high-protein amaranth starch granules with a volume mean diameter of 1.2 μm and polydispersity of 1.08,²⁴ and labeled as Unmodified.

Bulk Synthesis of Janus Particles via the Wax Pickering Emulsion Method. The wax Pickering approach we used to make Janus particles was customized from a method first proposed by Hong, Granick and Jiang (Figure 1A). ¹⁴ A reaction vessel (Figure 1B,C) was designed to facilitate the method, with a bottom compartment of 1.2 L capacity where the emulsion forms, and a top compartment of the same capacity that can be attached to add a reagent as the reaction progresses. The reagent flow to the emulsion is controlled by adjusting the stopcock at the bottom. This method has been validated to assess fitness of purpose (Sections S1 and S2, Figures S1–S3, under Supporting Information).

Preparation of Janus OSA-modified Amaranth Starch. Unmodified amaranth starch (4 g) was dispersed in 100 mL deionized water inside a 200 mL beaker and sonicated for 15 min. The beaker and its contents were then heated in a water bath at 60 °C [Figure 1A(i)]. When the starch dispersion reached 59-60 °C, 40 g of melted paraffin wax (1:10 w/w starch/wax) was added dropwise, homogenizing the mixture at 6000 rpm for 4 min using a high-speed homogenizer (IKA T25 digital Ultra Turrax, Germany) with a S25N-18G dispersing tool [Figure 1A(ii,iii)]. The beaker was then immediately submerged in an ice water bath and allowed to cool for 30 min. It was then removed from the ice water bath, placed in a room temperature water bath, and allowed to equilibrate for 1 h. Four batches of wax Pickering emulsions were made and then all four were transferred to the bottom compartment of the reaction vessel, and the top compartment was attached [Figure 1A(iv)]. An overhead stirrer was placed over the top compartment to make sure all reagents added mixed well during elution. The starch granules are half-submerged into solid wax and immobilized, leaving the other half of the granules exposed for subsequent OSA modification.

Once the reaction vessel is assembled, 400 mL of 1.5 mM NaOH was added to the top compartment of the reaction vessel to set the optimal alkaline pH for OSA reaction (pH 7.5–9.5). The overhead stirrer was turned on. The stopcock at the bottom was then opened to allow a flow of about 2-3 drops per second such that 400 mL of reagent eluted in 15–20 min [Figure 1A(v)]. After the NaOH solution has completely eluted from the top compartment to the bottom compartment, 400 mL of a 0.12 v/v % OSA solution in 30:70 EtOH/DI water was added into the top compartment and allowed to elute with stirring. After the OSA solution has completely eluted, the emulsions were treated to two washes of NaOH to readjust pH and then another treatment with OSA and then the process was repeated three times ending with a NaOH wash. Specifically, the following were added in this order: (1) 400 mL of 1.5 mM NaOH; (2) 400 mL of 1.5 mM NaOH; (3) 400 mL of 0.12% v/ v OSA; (4) 400 mL of 2.0 mM NaOH; (5) 400 mL of 2.0 mM NaOH; (6) 400 mL 0.12% v/v OSA; (7) 400 mL of 2.5 mM NaOH; (8) 400 mL of 2.0 mM NaOH; (9) 400 mL of 0.12% v/v OSA; (10) 400 mL of 2.0 mM NaOH; and (11) 400 mL of 1.5 M NaOH. After the final addition, the sample was neutralized by eluting 400 mL of 0.01% HCl. The sample was then washed twice with 400 mL of 30 v/v % EtOH in water, followed by 400 mL DI water, to remove residual OSA.

To isolate the Janus particles and remove the wax, the wax emulsions were then transferred into extraction thimbles and Soxhlet extraction with chloroform was performed for 9 h with an oil bath set at 105 $^{\circ}\text{C}.$ The resultant residue was then washed twice with acetone then with water, centrifuged at 5000g for 5 min each time to remove the supernatant, and then freeze-dried [Figure 1A(vi)]. The Janus particles produced using this method were labeled as Janus OSA. The yield per batch is approximately 25% or 1 g of Janus OSA starch.

Preparation of Control OSA-modified Amaranth Starch. Unmodified amaranth starch (4 g) was added to a beaker, then NaOH and OSA reagents were added in the same order as above while stirring, removing the reagents after every OSA addition using a centrifuge at 5000g for 5 min, then reconstituting the pellet with the next NaOH solution to be added. The control was then also neutralized with $0.01\,\mathrm{v/v}$ % HCl solution and washed with $30\,\mathrm{v/v}$ % EtOH twice and then water in the same way, then freeze-dried. The control produced using this method, a homogeneously OSA-modified starch, was labeled as Control OSA. Compared to the Janus OSA which is hydrophobic only on the side of the particle where OSA was added, the Control OSA is hydrophobic over its entire surface because of the homogeneous OSA addition.

Preparation of Janus Polymer-Modified Amaranth Starch. To verify the binary morphology, and estimate the Janus balance, of Janus particles produced using the 3D mask method, we also made Janus Polymer-modified starch. Janus OSA alone, unfortunately, cannot be used for this purpose, as they have small 1-2 nm OS groups that cannot be observed under scanning electron microscopy (SEM). Growing a large polymer on one-half side of a starch granule allows for the visualization of the binary morphology of Janus particles under SEM and allows for the estimation of Janus balance via SEM-energydispersive X-ray (EDX) and ImageJ.

The surface-initiated polymerization protocol used here was based on a method developed by Enayati and Abbaspourrad.^{25,26} First, 1 g unmodified amaranth starch was dispersed in 100 mL of acetonitrile (instead of water) in a beaker and sonicated for 15 min. Then, the beaker and its contents were heated in a water bath set at 60 °C [Figure 1A(i)]. When the starch dispersion reached 59–60 °C, 10 g of melted paraffin wax (1:10 w/w starch/wax) was added dropwise, homogenizing the mixture at 6000 rpm for 4 min using a high-speed homogenizer (IKA T25 digital Ultra Turrax, Germany) with a S25N-18G dispersing tool [Figure 1A(ii,iii)]. The beaker was then immediately submerged in an ice water bath and allowed to cool for 30 min. After which it was removed from the ice bath and poured into the top compartment of the assembled reaction vessel with stopcock closed. In making the wax emulsions in water to make the Janus OSA, we placed the emulsions in the bottom compartment because the emulsions would cream up, allowing the elution of reagents through it by opening the stopcock; in making wax emulsions in acetonitrile to make the Janus polymer particles, the emulsions would sediment due to the low density of acetonitrile, so it was necessary to place the emulsions on the top compartment rather than the bottom compartment, to prevent them from leaking out through the stopcock of the bottom compartment. At this point, the starch granules are now half-submerged into solid wax such that the other half is exposed and modifiable with APTMAC (a nitrogen-rich polymer) [Figure 1A(v)].

First, the initiator was attached as follows: the reaction vessel and all reagents were placed in a cold room at 4 °C for 1 h. Once equilibrated, a solution of bromopropionyl bromide (174 µL, 1.66 mmol) in acetonitrile (35.0 mL) containing triethylamine (NEt₃, 232 μ L, 1.66 mmol) was added to the top compartment and allowed to elute by opening the stopcock. After the solution has completely immersed the wax emulsion, the stopcock was closed, and the reaction was allowed to stand for 1 h at 4 °C and then an additional 2 h at room temperature. Excess water was then added to the top compartment and allowed to drain through the open stopcock to wash the emulsion.

After the initiator has been attached, surface-initiated Cu (0)mediated reversible radical polymerization was then performed via a "grafting from" approach. A solution of 75.0 w/w % APTMAC (9.24 mL) in water (27.7 mL) containing Me₆-TREN (44.4 μ L) was deoxygenated for 30 min at 20 °C by N₂ bubbling. Nanosize Cu(0) (25 nm, 10.56 mg) was added, and the mixture was sonicated for 1 min to disperse the copper. This mixture was then added to the reaction vessel and allowed to elute through the wax emulsion containing 1.0 g of previously initiator-functionalized amaranth starch. The stopcock was then closed, and the reaction was allowed to stand at room temperature for 4 h. Afterward, to isolate the Janus polymer particles and remove the wax, the wax emulsions were transferred into an extraction thimble, and Soxhlet extraction with chloroform was performed for 9 h with an oil bath set at 105 °C. The residue was then washed twice with acetone and then with water, centrifuging at 5000g for 5 min each time to remove the supernatant, then freeze-dried [Figure 1A(vi)]. The Janus particles produced were labeled as Janus Polymer.

Preparation of Control Polymer-Modified Amaranth Starch. The polymer control was prepared in parallel by placing 1 g unmodified amaranth starch in a beaker in a cold room, adding the reagents for initiator attachment in the same amounts as above, and then stirring for 1 h at 4 °C, then 2 h at room temperature. The solid was then washed three times with water, removing the supernatant each time after centrifugation at 5000g for 5 min. After washing, the pellet was transferred to a round bottom flask, and the reagents for polymerization were added in the same amounts. The reaction was stirred at room

temperature for 4 h. The solid was washed with water three times, centrifuging at 5000g for 5 min between each wash, and then freezedried. The control prepared using this method was labeled as Control Polymer. Compared to the Janus Polymer where only one side of the starch granule has polymer brushes attached (with the other half devoid of polymer brushes), the Control Polymer has polymer brushes over the starch granule's entire surface.

Janus Morphology and Janus Balance by SEM and EDX. To visualize the binary morphology of Janus particles produced via the wax Pickering emulsion method, the Janus Polymer was mounted on a silicon wafer atop an SEM stub and sputter-coated with carbon then imaged using a Zeis Gemini 500 field emission SEM. The same was done for the unmodified amaranth starch and the Control Polymer amaranth starch for comparison.

To measure, experimentally, the Janus balance of the Janus Polymer, or % coverage of polymer on the surface of the amaranth starch granule, nitrogen density maps were taken by EDX of 20 random Janus Polymer particles, using an aperture size of 60 μ m and electron beam of 7.5 kV. Each image was then processed using ImageJ 1.52p, using a set algorithm to remove noise and estimate for Janus balance: The image was first translated into an 8-bit B/W binary image. The brightness/ contrast was adjusted to remove noise. To remove any remaining noise, the image was de-speckled, outliers were removed and eroded, and holes were filled. The Janus nitrogen area was then divided over the total area of the particle to give the Janus balance. Then the average and standard deviation of the 20 individual Janus balances were calculated (experimental value). This randomized technique used to measure average Janus balance has been validated via simulations (Section S3, Figures S4 and S5, under Supporting Information).

Attenuated Total Reflectance-Fourier Transform Infrared **Spectroscopy.** The attenuated total reflectance (ATR)-Fourier transform infrared spectroscopy (FTIR) spectra of the unmodified, Janus OSA, and Control OSA amaranth starch were obtained using an ATR-FTIR Shimadzu Affinity-1S, to verify that ester bonds were formed due to reaction with OSA. The $400-4000~\text{cm}^{-1}$ region was scanned in transmittance mode with 2 cm⁻¹ resolution and 60 scans.

Nuclear Magnetic Resonance Microscopy. To measure OSA degree of substitution (DS), ¹H nuclear magnetic resonance (NMR) spectroscopy of the unmodified, Janus OSA, and Control OSA amaranth starch was done at 50 °C using a Bruker AV-500 NMR spectrometer. The starch samples were prepared by dissolving 50 mg in 1 mL D₂O, and heating at 90 °C for 2 h before analysis. The DS was estimated using the following equation:

degree of substitution (DS) =
$$\frac{\frac{A_{\text{OSA}}}{3}}{A_{\text{STARCH}}}$$
 (1)

where A_{OSA} refers to the area under the peak assigned to the methyl protons of OSA (1.2 ppm), and A_{STARCH} refers to the area under the peak assigned to the equatorial proton of the anhydroglucose unit of starch (5.7 ppm).²⁷ The DS was estimated in duplicate.

X-ray Diffraction. X-ray diffraction (XRD) analyses of the unmodified, Janus OSA, and Control OSA amaranth starch were performed using a Bruker D8 ADVANCE ECO powder diffractometer (Billerica, MA) to estimate crystallinity and to check whether unintended gelatinization occurred during the wax Pickering emulsion method. The powder samples were run from 5 to 60° under continuous scan at a step size of 0.026 with 2θ min⁻¹. The relative crystallinity was calculated as follows:^{28,2}

relative crystallinity (C %) =
$$\frac{A_c}{(A_c + A_a)} \times 100\%$$
 (2)

where A_c is total area due to the crystalline peaks, and A_a is the total area due to the amorphous peaks.

Differential Scanning Calorimetry. The differential scanning calorimetry (DSC) profiles of the unmodified, Janus OSA, and Control OSA amaranth starch were generated using a TA Q1000 modulated differential scanning calorimeter (Delaware, USA) to corroborate crystallinity data from XRD by measuring gelatinization temperature and enthalpy. A 1:5 w/w sample-to-water ratio was used, and the profile was taken from 30 to 90 $^{\circ}\text{C}$ at a heating rate of 10 $^{\circ}\text{C/min}.$

Self-Assembly via Optical Microscopy. Interparticle self-assembly was investigated via a single-blind experiment using an optical microscope. One scientist weighed 2 mg each of the unmodified, Janus OSA, and Control OSA amaranth starch, and 3 mL of DI water was added to each. The samples were then vortexed for 2 min, sonicated for 2–5 min, and mixed in a vertical rotator for 30 min. The samples were then handed to a second scientist, unaware of the identity of the samples, who then placed a 20 μ L aliquot of each sample on a coverslip, allowed them to settle for 1 min, then took pictures using a Leica Model DMIL LED microscope (Germany) with fast camera at 100× magnification. For each sample, over a span of 2 min, 20 random images were taken in a series from left to right and from top to bottom, covering approximately a 500 × 500 μ m² area and approximately 1000+ discrete granules or aggregates.

All images were then processed using ImageJ 1.52p to automatically generate the corresponding areas of each discrete granule or discrete aggregate. These areas were then pooled into five different categories by size, as shown in Table 1. The relative distribution of each aggregate category in terms of total area was then plotted in a bar graph using Origin Pro 9.7.5.184 (2020b).

Table 1. Different Categories by Size of Self-Assembled Particles

category	description	area μm^2
1. no aggregates	granules appear discrete and separate	0.6-2
2. 2- or 3- granule clusters (dimers and trimers)	2 or 3 granules appear to be bound together or touching	2-6
3. small wormlike strings	multiple granules form small, irregular, string-like aggregates	<50
4. large wormlike strings	multiple granules form large, irregular, string-like aggregates	50-100
5. supermicelles	multiple granules form a large , almost-spherical aggregate	>100

Critical Caking Concentration. To investigate thickening ability, the critical caking concentration (CCC) of the unmodified, Janus OSA, and Control OSA amaranth starch were measured in triplicate using a Buchner funnel filtration method: 1 g of dry starch was placed in a 15 mL tube, to which 9 mL of DI water was added. The tubes were vortexed for 2 min, sonicated for 2 min, and mixed in a vertical rotator for 30 min. They were then poured onto a 1.2 μ m-pore-size microfiber filter inside a Buchner funnel, and a 50 kPa vacuum pressure was applied until a wet starch cake was formed on the filter and no unadsorbed water remained on top of the cake, that is, the Buchner funnel can be turned upside down and no water will flow down the sides. The critical caking concentration was calculated using the following equation:

critical caking concentration =
$$\frac{\text{wt of dry starch}}{\text{wt of wet cake}} \times 100\%$$
 (3)

Water-Holding Capacity. To verify the CCC data and assess shelf stability, the water-holding capacity (WHC) of the unmodified, Janus OSA, and Control OSA amaranth starch were measured in triplicate using a modified centrifugation method based on Singh et al.³⁰ and Azfaralariff et al.³¹ Specifically, 1 g of sample was placed in a 15 mL centrifuge tube, to which 9 mL of DI water was added. The tubes were vortexed for 2 min, sonicated for 5 min, and mixed in a vertical rotator for 1 h. They were then centrifuged at 3000g for 10 min, the supernatants were decanted, any remaining water drained for 10 min, and the sediment was weighed before and after freeze-drying for 24 h. The water-holding capacity was calculated using the following equation:

water-holding capacity

$$= \frac{\text{wt of wet sediment} - \text{wt of dried sediment}}{\text{wt of dried sediment}} \times 100\%$$
 (4)

Rheology. Viscosity at a Single Concentration. To compare the actual thickening ability of Janus OSA to Control OSA and unmodified amaranth starch, the viscosity of 20 w/w % dispersions in water of each was measured in triplicate using a TA DHR3 rotational rheometer (Delaware, USA) and using a 20 mm parallel plate and 500 μ m gap size. The dispersions were vortexed for 2 min, sonicated for 5 min, and mixed in a vertical rotator for 30 min prior to measurement. Very viscous dispersions that could not be mixed by vortex were mixed manually using a spatula prior to sonication. The viscosity was measured at 25 °C using a $0.02-100 \text{ s}^{-1}$ shear rate sweep.

Viscosity and Moduli at Different Concentrations. To assess if Janus OSA can reduce the amount of starch needed to achieve the same viscosity, the viscosity at different concentrations in water was tested for the unmodified, Janus OSA, and Control OSA amaranth starch. The moduli at different concentrations were likewise measured to compare gel firmness, strength, and stability.

The viscosity, storage moduli, and loss moduli at different concentrations in water of the unmodified, Janus OSA, and Control OSA amaranth starch were measured in triplicate at 25 °C using a TA DHR3 rotational rheometer and using a 20 mm parallel plate and 500 μ m gap size. For each sample, four different concentrations (w/w) were prepared at 2.5, 5, 7.5, and 10% below the CCC for that sample. The dispersions were vortexed for 2 min, sonicated for 5 min, and mixed in a vertical rotator for 30 min prior to measurement. Very viscous dispersions that could not be mixed by vortex were mixed manually using a spatula prior to sonication. The following tests were then performed: oscillation strain sweep at 1 Hz frequency, at 0.1-10% strain; oscillation frequency sweep at 0.1% strain, at 0.01-100 Hz frequency; and shear rate sweep at 0.02-100 s⁻¹ shear rate. The yield point was estimated to be the point at which G' starts to decline by 5% or more, and the flow point as the point at which the G' and G'' values intersect and G'' > G'

Emulsifying Ability via Droplet Size and El. The emulsifying abilities of unmodified, Janus OSA, and Control OSA amaranth starch were studied by preparing in triplicate 30 v/v % O/W emulsions using 0.67 g starch/mL corn oil and a pH 6.5 buffer. The emulsions were made by homogenization at 11,000 rpm for 4 min using a high-speed homogenizer (IKA T25 digital Ultra Turrax, Germany) with an S25N-18G dispersing tool. The emulsion index was measured using the following equation:

emulsion index =
$$\frac{V_{\rm E}}{V_{\rm T}}$$
 (5)

where $V_{\rm E}$ is the volume of the emulsion (upper cream layer) and $V_{\rm T}$ is the total volume of the whole sample (including all layers or phases). Likewise, the emulsion droplet size was measured by taking images of the emulsion droplets using an optical microscope at 4× magnification and then using ImageJ to calculate the diameter di of N number of particles, where N > 200, then computing for volume mean diameter (d_{43}) and polydispersity index (PDI) using the following equations: 33

$$d_{43} = \frac{\sum di^4}{\sum di^3}$$
 (6)

$$PDI = \frac{d_{43}}{\sum \frac{di}{N}} \tag{7}$$

Interfacial Tension by Goniometry. To study emulsifying ability further, the interfacial tension between corn oil and water in the presence of unmodified, Janus OSA, and Control OSA amaranth starch was measured using a pendant drop method based on Zhao et al. 34 A 30 μ L droplet of a starch dispersion (1 w/w %) in DI water was formed at the tip of a syringe and submerged into corn oil. The interfacial tension was then measured using an advanced goniometer (model 500-U1, rame-hart instrument co., NJ, USA) at 10 s intervals over 1000 s.

Crude Protein Analysis. To assess how much protein is retained in the starch after Janus synthesis using OSA, which may have implications for thickening and emulsifying properties, the unmodified, the Janus OSA, and Control OSA amaranth starch were tested in triplicate for

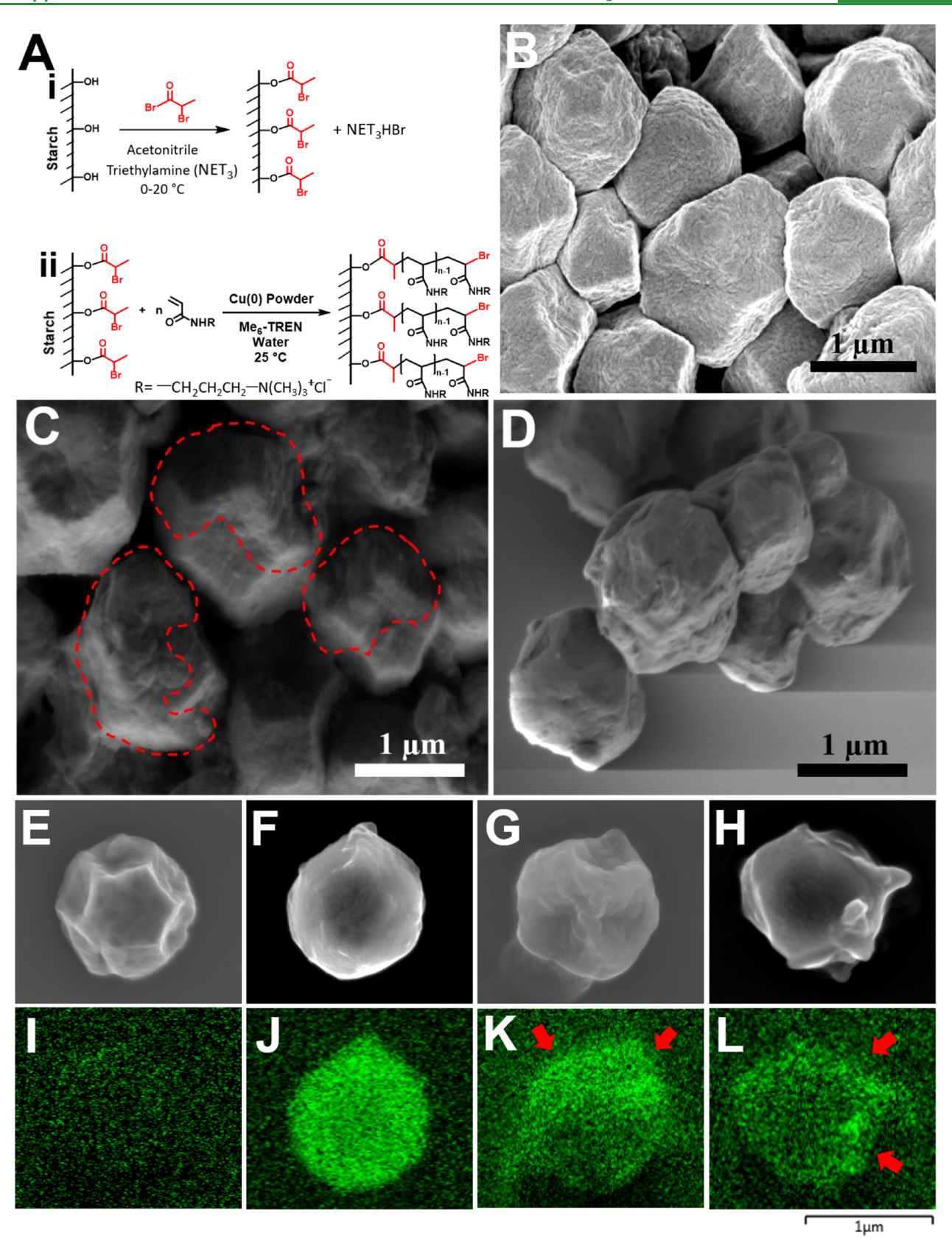


Figure 2. Janus Polymer amaranth starch morphology. (A) Reaction scheme of "grafting from" attachment of APTMAC onto starch. Field emission SEM images of (B) unmodified amaranth starch, (C) Janus Polymer amaranth starch, with polymer patches highlighted with red dotted lines, and (D) Control Polymer amaranth starch. Field emission SEM images (upper panel) and SEM-EDX nitrogen density maps (lower panel) of a single granule of unmodified (E,I), Control Polymer (F,J), and two Janus Polymer starch granules (G,K; H,L), respectively. Scale bar is 1 μ m for (E-L).

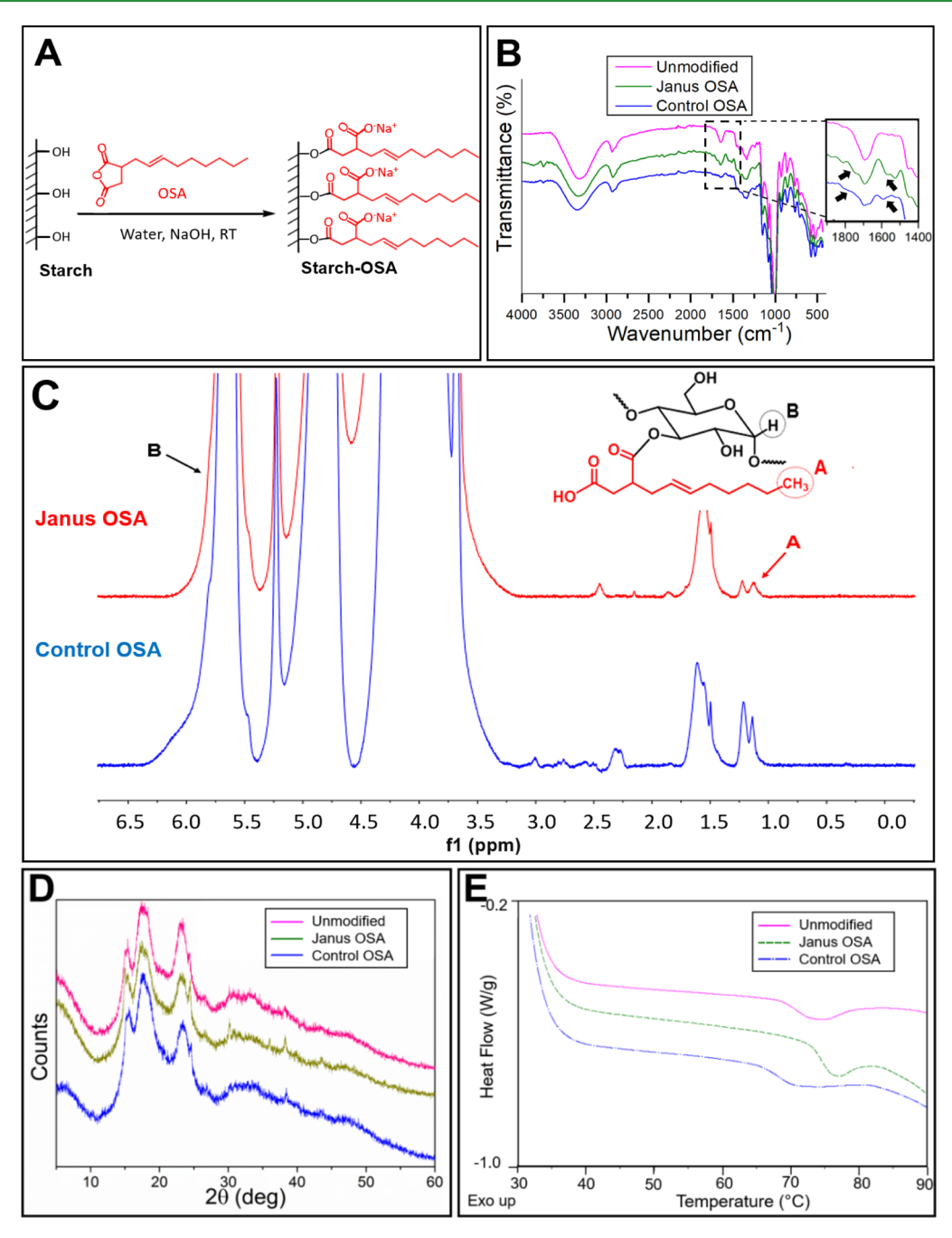


Figure 3. Janus OSA amaranth starch characterization. (A) reaction scheme of OSA reaction with starch; (B) ATR-FTIR spectra, (C) NMR spectra, (D) X-ray diffraction patterns, and (E) DSC profiles of unmodified, Janus OSA, and Control OSA amaranth starch.

crude protein content using AOAC 992.23 (combustion method) and a nitrogen-to-protein conversion factor of 6.25 on a % dry basis.³⁵

Statistical Analysis. Triplicate analyses were performed (unless otherwise stated), and analysis of variance (ANOVA) and t-tests (P < 0.05) were performed where appropriate using Microsoft Excel.

RESULTS AND DISCUSSIONS

The 3D wax Pickering emulsion method developed here (Figure 1) was found to successfully produce intact Janus particles from amaranth starch in bulk (see Section S1, Figures S1 and S2, for the results of the method validation conducted to assess fitness of purpose). Two kinds of Janus particles were made using this method, Janus Polymer amaranth starch and Janus OSA amaranth starch. We used the Janus Polymer to verify and

quantify the binary morphology of Janus particles produced using this method. Because the Janus Polymer starch has large brushes of nitrogen-rich polymer grown on one-half side, they can be visualized by SEM-EDX to verify their binary morphology, and these images in turn can be used to estimate their Janus balance. The Janus OSA cannot be used for this purpose because they only have small 1–2 nm OS groups that cannot be visualized by SEM. We used the Janus OSA instead to demonstrate that we can employ our method to make a prototype starch ingredient for the food industry, using a Food and Drug Administration (FDA)-approved OSA reagent. Janus OSA, which are hydrophobic/hydrophilic Janus particles, were characterized by ATR-FTIR, NMR, XRD, and DSC to confirm and quantify the OSA reaction and ensure that intact

(nonbroken or nongelatinized) Janus particles were made. Then, to demonstrate their potential applications in food, their self-assembly behavior, critical caking concentration, water-holding capacity, rheology, surface activity, and protein content were investigated as well.

Janus Polymer Amaranth Starch. Morphology by Polymerization and SEM-EDX. A nitrogen-rich polymer (APTMAC) was grown on one side of the amaranth starch to produce Janus Polymer amaranth starch with polymer chains long enough to visually verify that our method can produce Janus particles with a binary morphology (Figure 2A). Under SEM, an unmodified amaranth starch granule appears polygonal with flat surfaces and sharp edges (Figure 2B). The SEM images of the Janus Polymer showed an irregular and rounded side due to the polymer growth and a sharp-edged side that was flatter and similar to unmodified starch (Figure 2C). The Control Polymer amaranth starch, or the starch granule fully coated with polymer on its entire surface, looks more irregular and rounded over its entire surface, as expected (Figure 2D).

To further confirm the binary morphology of the Janus particles, SEM-EDX nitrogen density maps of individual Janus Polymer starch granules were also obtained (Figure 2E-L). Unmodified amaranth starch (Figure 2E) does not show any appreciable nitrogen on its surface (Figure 2I). The Control Polymer starch (Figure 2F) shows an intense nitrogen density evenly distributed over its entire surface, which can be attributed to the nitrogen-rich polymer being evenly distributed over its entire surface (Figure 2J). For comparison, two Janus Polymer amaranth starch granules are shown (Figure 2G,H) with their respective nitrogen density maps (Figure 2K,L). Unlike the Control Polymer, the Janus Polymer particles have an intense nitrogen density on only one side, which indicates that Janus particles were successfully produced. To show that this approach produces Janus particles in bulk, and not just in isolated instances, an SEM image of a group of Janus Polymer particles is shown in Figure S3A, with their polymer halves highlighted in red (Figure S3B under Supporting Information).

Janus Balance by Polymerization and SEM—EDX. Janus balance is a critical property of Janus particles that can dictate their self-assembly behavior. The average Janus balance (or polymer coverage) of Janus particles made using our method was estimated to be 49%, with a standard deviation of 21%, confirming their binary morphology (see Section S3 under Supporting Information for validation of the technique used to estimate this value).

Janus OSA Amaranth Starch. Attenuated Total Reflectance-Fourier Transform Infrared Spectroscopy. When starch is modified with OSA, in basic conditions, alkoxide ions on the starch surface will attack the OSA's anhydride as a nucleophile, resulting in the attachment of a hydrophobic octenyl group via an ester bond (Figure 3A).³⁶ Prior to OSA modification, the unmodified starch exhibited characteristic bands that have been assigned to native starch in the literature: a broad O-H vibration at 3400 cm⁻¹; C-H stretching at 2915 cm⁻¹; adsorbed water bending vibration at 1640 cm⁻¹; C-H deformation peaks at 1360-1420 cm⁻¹; and a fingerprint region at 1000–1200 cm⁻¹ for C–O stretching (Figure 3B).³⁷ After OSA modification, for the Control OSA, starch granules homogeneously covered by OS octenyl groups over their entire surface, a strong peak appears at 1730 cm⁻¹ for C=O stretching vibration, which confirms that an ester bond was formed between OSA and starch. Another small peak that appears at 1560 cm⁻¹ for the asymmetric stretching vibration of the

carboxylate group of OSA further confirms the reaction. ^{37,38} Likewise, the Janus OSA starch has the same peaks at 1730 and 1560 cm⁻¹. The Control OSA's relative peak intensity ratio for the ester bond (C=O [1730 cm⁻¹]/C-H [2915 cm⁻¹]) is larger than that of Janus OSA starch. This suggests that the Control OSA has a higher degree of OS substitution than Janus OSA, which is what would be expected if the Janus OSA only has half of its surface covered with OS groups.

OSA DS by NMR. Proton NMR was used to estimate that the Janus OSA starch and Control OSA starch have DS values of 0.0018 ± 0.0001 and 0.0027 ± 0.0001 , respectively. Peaks at 3-6 and 0.8-2.5 ppm are attributed to starch and OSA, respectively (Figure 3C).³⁹ The NMR spectra of Janus OSA starch shows peak A at ~1.1 ppm, representing the OSA methyl protons, and peak B at ~5.6 ppm, representing the starch equatorial proton, from which the DS was estimated using the relative areas under the curve of these peaks per eq 1 (Figure 3C, top).²⁷ The Janus OSA starch has a DS about 68% that of the Control OSA starch (Figure 3C, red vs. blue), which aligns with the results from the ATR-FTIR spectra (Figure 3B), and is what would be expected if only about half of the surface of Janus OSA starch is covered with OS groups. This 68% result for Janus OSA also aligns approximately with the 49% Janus balance estimated for the Janus Polymer in the previous section.

X-ray Diffraction. XRD was used to check that the Janus starch particles remain intact and retain much of their semicrystalline structure during the synthesis process (Figure 3D). The relative crystallinity of the unmodified, Janus OSA, and Control OSA amaranth starch were calculated to be 33.0, 28.1, and 28.9%, respectively. The unmodified starch has sharp peaks at 15, 17.5, and 23.5°, which indicates A-type crystallinity typical for amaranth starch. After Janus synthesis, these peaks remain sharp, showing only a slight reduction in crystallinity of about 15%. This indicates that much of the native starch's crystallinity was retained during synthesis and suggests that the Janus particles that were synthesized remained intact.

Differential Scanning Calorimetry. The DSC profiles of the unmodified, Janus OSA, and Control OSA amaranth starch show endotherms with peak gelatinization temperatures (T_p) at 73.7 (± 0.0), 76.6 (± 0.2), and 70.8 (± 0.3) °C, with corresponding gelatinization enthalpies (ΔH_g) of 2.3 (± 0.4), 1.80 (± 0.04), and 2.0 (± 0.1) J/g, respectively (Figure 3E). Homogeneous modification of starch with OSA results in the reduction of both the peak gelatinization temperature and the gelatinization enthalpy, indicating that the hydrogen bonding within the granule has been disrupted and weakened by the addition of bulky, hydrophobic octenyl groups that also contain a negative charge, which then helps the granules swell at a lower temperature, requiring less energy to disrupt the semicrystalline structure.⁴¹ Following this trend, the unmodified amaranth starch gelatinizes at 73.7 °C, whereas Control OSA gelatinizes at a lower temperature of 70.8 °C, with a slightly lower enthalpy of gelatinization due to the OSA modification, as reported in the literature. 41 Conversely, the Janus OSA gelatinizes at a slightly higher temperature of 76.6 °C than both unmodified and Control OSA, with a slightly lower enthalpy of gelatinization than both. It is unclear why the peak gelatinization temperature of Janus OSA is higher, but the difference may be due to the high viscosity of the Janus OSA dispersion in water, which can slow the diffusion of heat and therefore shift the observed peak gelatinization temperature. It may also be attributed to how Janus OSA particles can self-assemble and trap water, lowering the amount of free water that can participate in gelatinization,

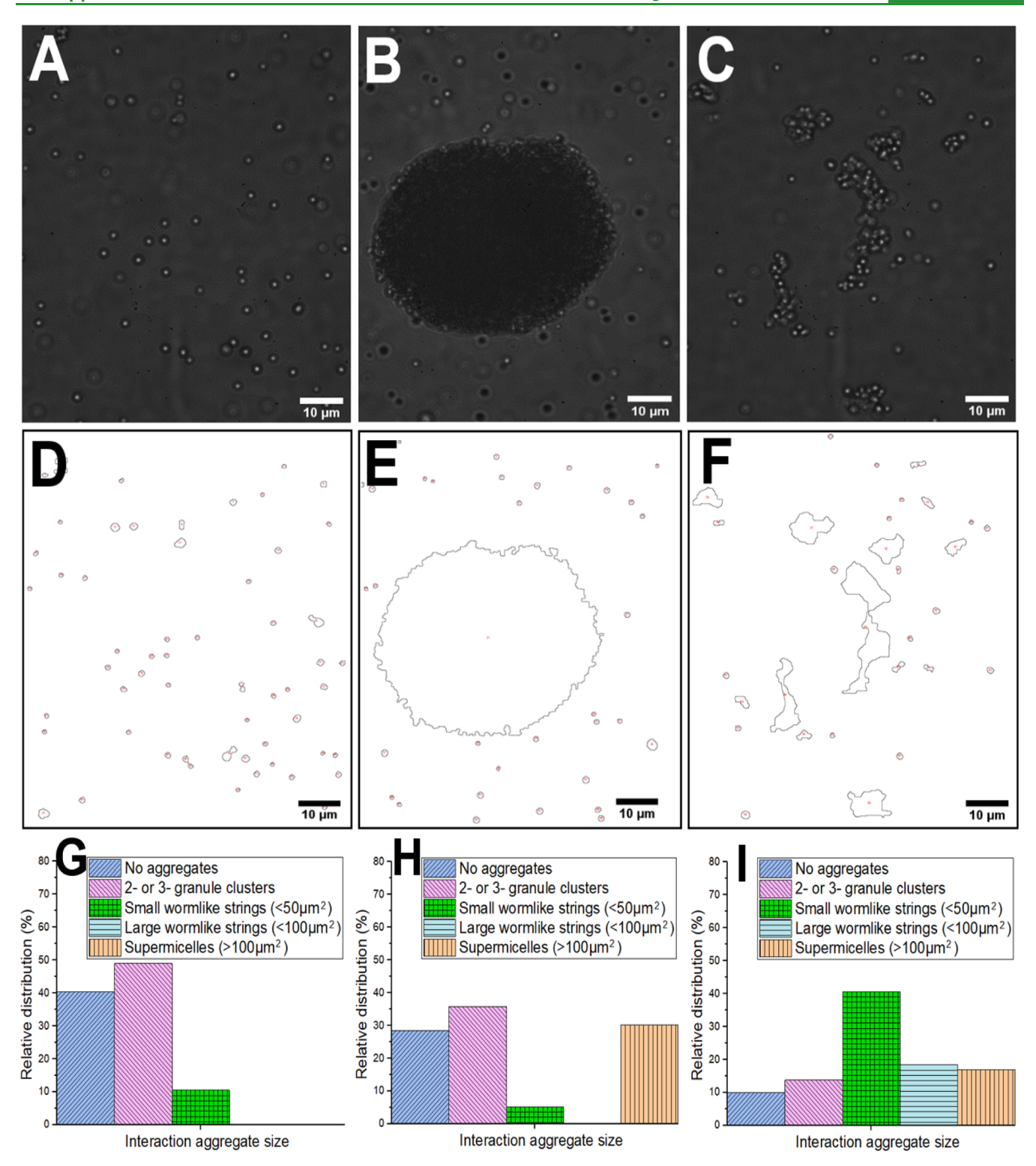


Figure 4. Self-assembly of Janus OSA amaranth starch particles. Representative intergranule self-assembly in water of (A) unmodified, (B) Control OSA, and (C) Janus OSA amaranth starch, taken using an optical microscope at 100× magnification. Their corresponding aggregate area outlines after processing via ImageJ are shown for (D) unmodified, (E) Control OSA, and (F) Janus OSA. Relative distributions of interparticle aggregate sizes, taken out of 20 random images and 1000+ aggregates/elements each, are shown for (G) unmodified, (H) Control OSA, and (I) Janus OSA. The "2- or 3-granule clusters" category refers to dimers or trimers. A note on the relative distribution: to generate them, the cross-sectional area was used and not the volume; thus, the distributions will necessarily give more weight to smaller aggregates than to larger aggregates, and so the true distribution will probably consist of a larger percentage of larger aggregates than what is shown.

therefore again shifting the gelatinization temperature.²⁷ As for the lower enthalpy of gelatinization of Janus OSA compared to both unmodified starch and Control OSA, the reaction of the

starch with OSA and the subsequent chloroform washing during synthesis gently disrupts the hydrogen bonding within the starch structure and thus lowers the amount of energy required for

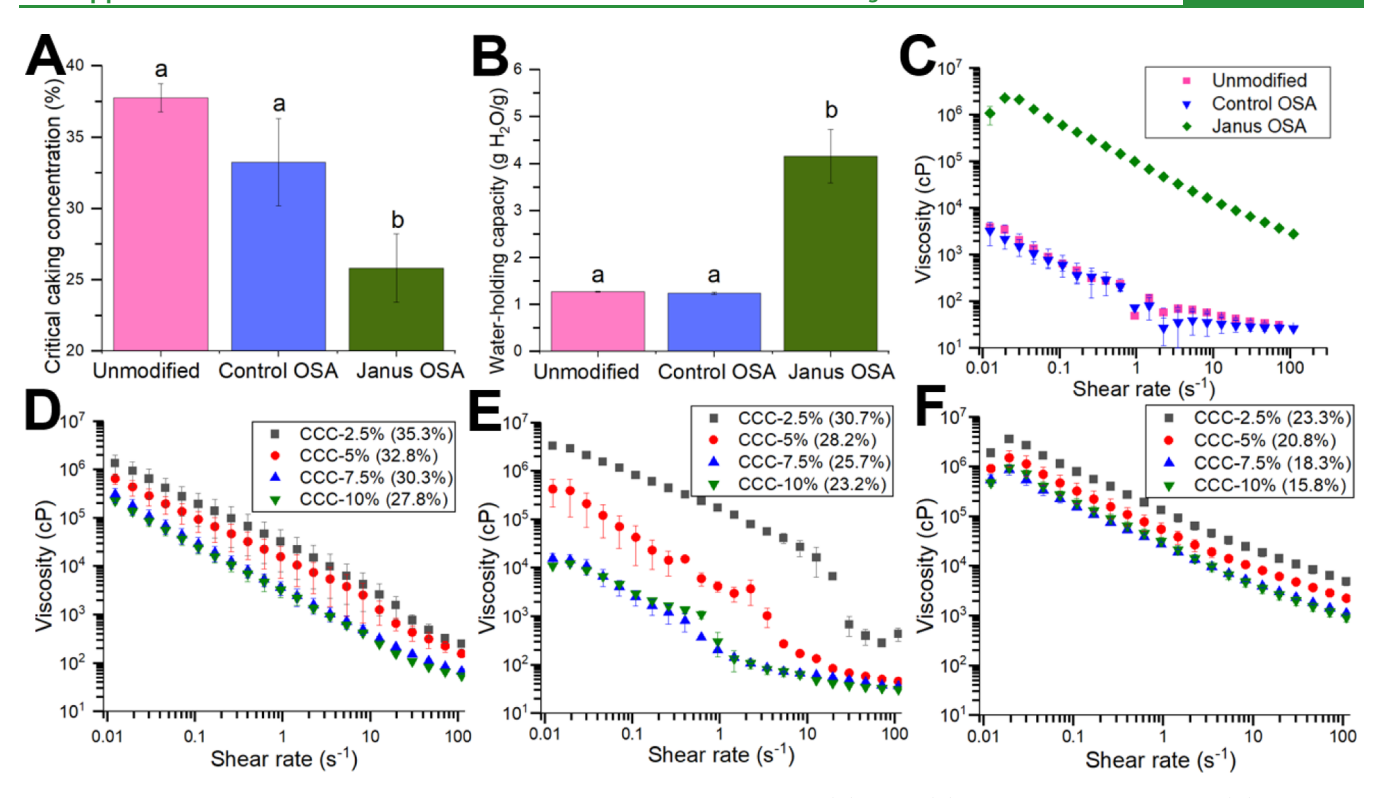


Figure 5. Physicochemical properties of Janus OSA amaranth starch: thickening ability. (A) CCC, (B) water-holding capacity, and (C) viscosity at 20% (w/w) concentration for unmodified, Control OSA, and Janus OSA amaranth starch. Viscosity at four concentrations incrementally lower than the CCC (-2.5, -5, -7.5, and -10%) for (D) unmodified, (E) Control OSA, and (F) Janus OSA amaranth starch. In (A,B), data points tagged with different letters are statistically different (p < 0.05). Error bars refer to standard deviation.

gelatinization. Overall, the DSC data show that the granule crystallinity of the Janus OSA was only slightly disrupted during Janus synthesis, which corroborates the XRD data from the previous section and suggests intact Janus particles.

Self-Assembly Observed by Optical Microscopy. Representative images were taken to show the self-assembly in water of unmodified, Control OSA, and Janus OSA amaranth starch (Figure 4A–C). These images were processed to calculate for the area of each discrete element or aggregate (Figure 4D–F), and then tabulated in a bar graph to give their relative size distribution by category (Figure 4G–I).

Unmodified amaranth starch in water exists mostly as discrete granules and 2- or 3-granule clusters (90% of all interactions) with no large aggregates because there is no strong attraction between granules to cause any appreciable interactions (Figure 4A,G). When hydrophobic groups are homogeneously attached over the entire surface of starch granules to make the Control OSA, strong hydrophobic intergranule interactions bring about the formation of very large aggregates or supermicelles (>30% of all interactions) (Figure 4B,H). For Janus OSA, where only onehalf of the granule was made hydrophobic by OSA modification, the particles mostly interact to form irregular, wormlike strings in water (>59% of all interactions), plus some small micelles and some dimers and trimers (Figure 4C,I). The other side of the Janus OSA particle that was not modified by OSA and is thus considered hydrophilic by comparison may still contain residual proteins that may impart some level of hydrophobicity. Although based on the self-assembly, they do not appear to be appreciable enough to mimic the behavior of the Control OSA.

These self-assembly results generally agree with our previous work on starch-based Janus particles produced via a 2D mask approach.²¹ A modeling study has also shown that if a Janus

particle has an attractive patch that covers 50-60% of the particle's surface, wormlike strings will be formed, and that if the patch covers more than 89% of the surface, which closely resembles our Control OSA, larger aggregates or supermicelles will be formed instead.⁴² It is believed that Janus particles selfassemble into these wormlike strings because one Janus particle will first attach to a second Janus particle if their attractive patches are aligned, and then this second particle will then attach to a third particle if their attractive patches are again available to each other, and then to a fourth particle, and so on, thus forming a wormlike string.⁴³ For the Control OSA, because they are homogeneously hydrophobic over their entire surface, intergranule attraction is multidirectional, so one granule attracts several granules surrounding it, and those in turn attract many more granules around them, thus forming much larger aggregates or supermicelles.

Critical Caking Concentration. The CCC measures the minimum concentration at which a starch dispersion starts to form a semisolid cake. The unmodified, Control OSA, and Janus OSA amaranth starch have critical caking concentrations of 38 ± 1 , 33 ± 3 , and $26 \pm 2\%$, respectively (Figure 5A). Although the difference between the CCC of the unmodified starch and that of the Control OSA is not statistically significant, the much lower CCC of the Janus OSA is statistically different from both (p < 0.05).

An effective thickener, or a material that even at low concentrations quickly thickens a dispersion, is expected to have a low CCC, whereas a less-effective thickener that requires a high concentration before it can thicken a dispersion is expected to have a high CCC. Because unmodified starch generally do not self-assemble, they will have an effective dispersed phase volume comparable to their actual granular

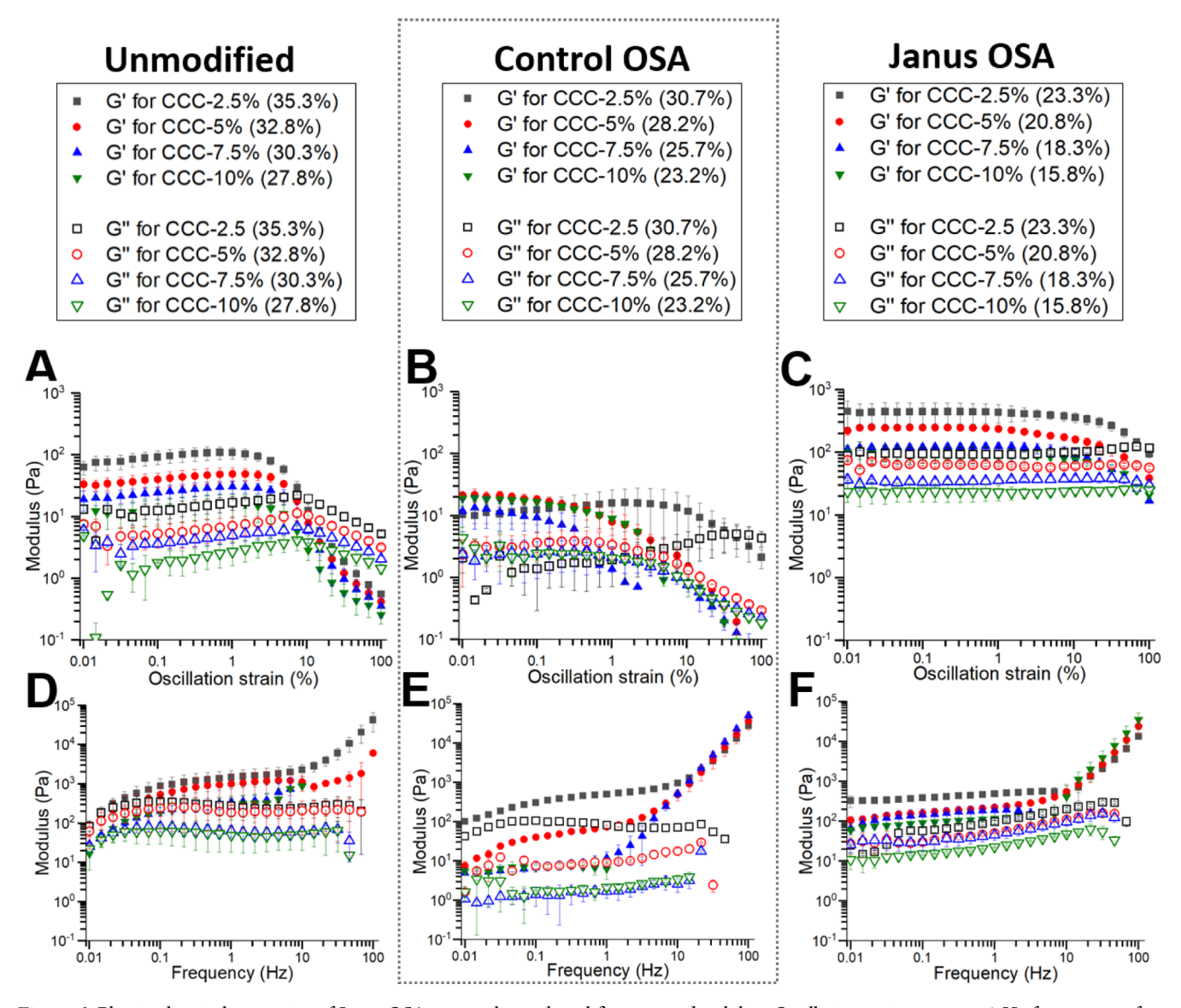


Figure 6. Physicochemical properties of Janus OSA amaranth starch: gel firmness and stability. Oscillation strain sweep at 1 Hz frequency at four concentrations incrementally lower than the CCC (-2.5, -5, -7.5, and -10 w/w %) for (A) unmodified, (B) Control OSA, and (C) Janus OSA amaranth starch. Oscillation frequency sweep at 0.1% strain at the same four concentrations for (D) unmodified, (E) Control OSA, and (F) Janus OSA amaranth starch.

volume and thus had a 38% CCC, which is typical for amaranth starch. Control OSA was observed to form large supermicelles (Figure 4B), so it is expected to have a slightly larger effective dispersed phase volume than the unmodified starch. This is because the spaces between the granules forming the supermicelles add to the effective dispersed phase, which gives it a slightly better thickening ability than the unmodified starch. Control OSA has an insignificantly lower CCC of 33% (p > 0.05).

Compared to both the unmodified starch and the Control OSA, however, the Janus OSA starch showed a much lower CCC (26%) that was statistically significant (p < 0.05). Because Janus OSA granules self-assemble into small or large wormlike strings that stretch out in different directions and can rotate in dispersion (Figure 4C), they can occupy a much larger effective dispersed phase volume than the actual dispersed phase volume that their constituent granules occupy. This larger effective dispersed phase volume allows them to form a network that can quickly thicken a solution even at low concentration. These

networks can also trap water between them, reducing water flow and increasing viscosity. These results indicate that Janus OSA particles have a much better thickening ability than both the unmodified starch and the Control OSA.

Water-Holding Capacity. WHC measures the ability of a material to bind or trap water, and can be a measure of a food's shelf stability. ⁴⁴ The more sites in a material that are available to either bind water molecules through hydrogen bonding, or to trap them, the larger the WHC. ³¹ The WHC of the unmodified, Control OSA, and Janus OSA amaranth starch were found to be 1.27 ± 0.01 , 1.24 ± 0.03 , and 4.1 ± 0.6 g H₂O/g starch, respectively (Figure 5B). Although the WHC of the unmodified starch and the Control OSA starch were not statistically different from each other, the WHC of the Janus OSA was found to be much larger than both, and the difference was statistically significant (p < 0.05).

The WHC of Janus OSA starch is almost four times higher than that of the unmodified starch and the Control OSA, indicating that Janus OSA starch binds and traps water much

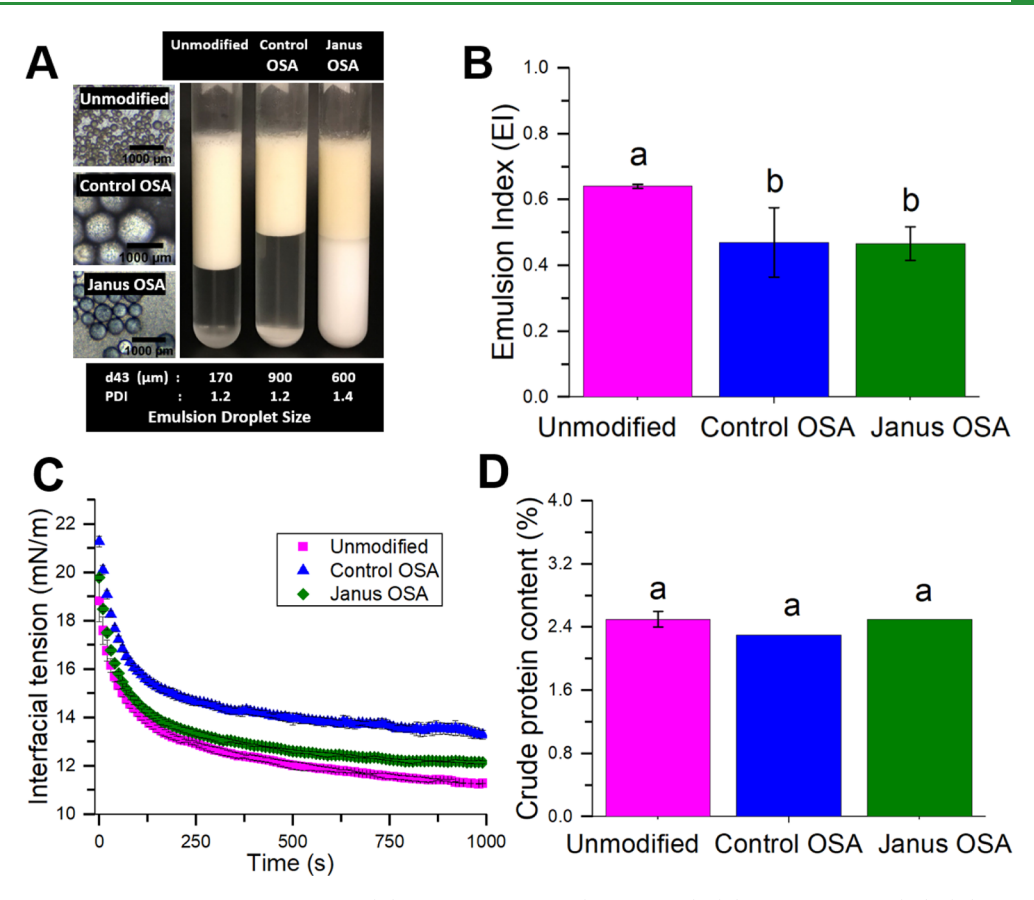


Figure 7. Surface activity of Janus OSA amaranth starch: (A) emulsifying ability (droplet size), (B) emulsion index (EI), (C) interfacial tension, and (D) crude protein content of unmodified, Control OSA, and Janus OSA amaranth starch. Data points tagged with different letters are statistically different (p < 0.05). Error bars refer to standard deviation.

more effectively. This greater WHC may again be attributed to the self-assembly of these Janus particles into wormlike strings, allowing the formation of a network that can trap more water molecules inside the network, which can lead to both a higher viscosity and a higher shelf stability as they restrict the flow of water molecules and prevent syneresis. Thus, based on the WHC data, Janus OSA starch is expected to have a better thickening ability and shelf stability than unmodified starch and Control OSA, a result which is supported by the previous section on CCC.

Viscosity at One Concentration. To compare the actual thickening abilities between the unmodified, Janus OSA, and Control OSA amaranth starch, their viscosities were measured at one concentration (20 w/w %). This concentration is high enough to allow us to see any viscosity effects due to intergranule interactions but still below the CCCs of all three samples. At all shear rates measured, from 0.01 to 100 s⁻¹, all samples showed shear-thinning behavior, but the viscosity of the Janus OSA was much higher by two or three orders of magnitude than those of both the unmodified starch and Control OSA (Figure 5C). If we take their viscosities at one shear rate (13 s⁻¹), the viscosity difference between the Janus OSA and the unmodified amaranth starch, and between Janus OSA and the Control OSA, are statistically significant (p < 0.05). Conversely, there is no statistically significant difference between the viscosity of the unmodified starch and that of Control OSA. These viscosity results concur with the CCC and the WHC results, which verifies that Janus OSA has a greater thickening ability than both

unmodified and Control OSA starch, due to their ability to self-assemble into wormlike strings in water.

Viscosity at Different Concentrations. To assess if the use of Janus OSA results in the reduction of the amount of starch needed to achieve the same viscosity, the viscosity profiles at $0.01-100~\rm s^{-1}$ shear rate of the unmodified, Control OSA, and Janus OSA amaranth starch at four concentrations below their CCC were recorded (Figure 5D–F). A comparable viscosity (at $\sim 10~\rm s^{-1}$) can be achieved using a 15.8% concentration of Janus OSA and a 35.3% concentration of unmodified starch in water. This suggests that we could reduce the amount of starch used in a formulation by $\sim 55\%$ if we use Janus OSA instead of unmodified starch to make lower-calorie food products.

Oscillatory Amplitude Sweep at Different Concentrations. To determine the linear viscoelastic region (LVR), amplitude sweeps were performed for unmodified, Control OSA, and Janus OSA amaranth starch at four concentrations below their CCCs (-2.5, -5, -7.5, and -10 wt %) (Figure 6A–C).

For all samples, at low strains, G' is larger than G'', where G' is the storage modulus (closed symbols) and G'' is the loss modulus (open symbols). This indicates that these samples are gel-like or viscoelastic solids at low strains. The region where G' is constant represents the LVR. However, at higher strains at a certain yield point, G' starts to decline, indicating that the network or gel structure starts to fracture, which defines the limit of the LVR. At even higher strains, the G' and G'' cross over at the flow point, at which point the solid gel has been sufficiently fractured that it starts to flow as a liquid. At comparable concentrations (27.8, 23.2, and 23.3% for unmodified, Control

OSA, and Janus OSA), the Janus OSA has G' values about 45 times higher than the unmodified starch and Control OSA, indicating that Janus OSA makes firmer or more elastic gels. In addition, for all samples, the length of the LVR decreases as concentration decreases, indicating how lower concentrations make gels that fracture more easily, but Janus OSA retains its long LVR even at lower concentrations. Likewise, at comparable concentrations, Janus OSA has an LVR (0.01-10.5% strain) that is, about 7 and 105 times longer than those of the unmodified (0.01-1.5% strain) and Control OSA (0.01-0.1% strain), respectively. This indicates that Janus OSA makes a much more stable or well-dispersed gel network or structure. Likewise, the flow point of the Janus OSA (68% strain) is about 9 times higher than that of the unmodified (7.4%) and 20 times higher than that of the Control OSA (3.3%), indicating that the network, or structure, formed by Janus OSA is much stronger and more resistant to breaking, likely due to Janus-specific, interparticle self-assembly, which suggests that Janus OSA may be used to make firmer food gels with better shelf stability.

Oscillatory Frequency Sweep at Different Concentrations. Within the LVR, oscillatory frequency sweeps at 0.1% strain and 0.01–100 Hz frequency were performed for the unmodified, Control OSA, and Janus OSA amaranth starch at the same four concentrations below their CCCs as in the previous section, to study the samples' degree of interparticle association and dispersion (Figure 6D–F). High frequencies simulate fast motion and low frequencies simulate slow motion or slow changes in stress, which provides information about the samples' structural stability.

The moduli of Janus OSA appear to be less affected by the frequency than both the unmodified and the Control OSA, which indicates that the Janus starch granules are more strongly associated with each other in a stable network and less likely to sediment, which may again indicate better shelf stability if used in a food product. At low frequencies, the G' and G'' of unmodified starch start to converge, which indicates that the undissociated, unmodified starch granules may start to sediment, thus making the gel flow more like a liquid. On the contrary, for both the Control OSA and Janus OSA, G' > G''even at low frequencies, which indicate that the particles remain dispersed and form a gel network due to interparticle hydrophobic interactions. In addition, at comparable concentrations, the G' for Janus OSA is about 2 and 50 times higher than those of the unmodified and Control OSA, respectively, indicating that Janus OSA again forms a firmer gel network, indicating better thickening and gelling ability.

Surface Activity. The surface activity of the Janus OSA starch was also tested because their amphiphilic nature could presumably give them improved emulsifying abilities. It was found that unmodified, Janus OSA, and Control OSA amaranth starch formed O/W emulsions with droplet sizes of 170, 900, and 600 μ m (with PDI's of 1.2, 1.2, 1.4), respectively (Figure 7A). These emulsions had emulsion indices of 0.64 \pm 0.01, 0.47 \pm 0.1, and 0.47 \pm 0.05, respectively (Figure 7B). The O/W interfacial tension was recorded over 1000 (Figure 7C).

An effective emulsifier is one that easily adsorbs onto the oil/water interface, effectively lowering the O/W interfacial tension, and promoting the formation of smaller oil droplets, which are also more stable over time because they are less prone to creaming according to Stokes' law. Because smaller droplets have a larger effective volume fraction, namely $(1 + \delta_x/r)^3$ times that of the actual volume fraction, where δ_x is the adsorbed starch layer thickness and r is droplet radius, effective emulsifiers

also give higher emulsion indices. 46,47 Typically, OSA modification of starch improves its emulsifying properties, in terms of smaller droplet sizes, larger emulsion indices, and lower interfacial tension. 48,49 Our results indicate the opposite trend, both Janus OSA and Control OSA starch appearing to be lesseffective emulsifiers than the unmodified starch. There are some possible explanations for this: first, typical OSA modifications are done on commercial, low-protein starches, so OSA modification increases their hydrophobicity and emulsifying ability. In our case, our unmodified amaranth starch is already high in protein and therefore already a good emulsifier (Figure 7D). Further modification with OSA may have increased its hydrophobicity even further, so much so that the increased intergranule attraction may have reduced the number of granules available to participate in oil droplet stabilization. This is particularly evident for Janus OSA, where they selfassemble in the water phase below the cream layer (see cloudy lower phase in Figure 7A, rightmost tube), making them unable to participate in emulsion stabilization. Thus, although theoretically, amphiphilic Janus particles are expected to be better emulsifiers than homogeneous particles, 50,51 it is possible that the Janus particles produced here exhibit such strong selfassembly that they prefer to form a network with each other in water rather than participate in oil/water stabilization (or they go into the oil phase entirely). This may explain why, without oil, these Janus OSA particles form a very strong network in water, in the process trapping water and increasing their effective dispersed phase volume and making them much more effective thickeners and gelling agents than the controls, as shown in the previous sections.

CONCLUSIONS AND POTENTIAL APPLICATIONS

In this study, we adapted and modified a scalable, 3D mask method for the bulk synthesis of Janus particles using starch, a natural biopolymer widely used in the food industry. This method can be used to produce Janus particles with about 49% Janus balance and to create, via OSA modification of one side (half) of the particle, hydrophobic/hydrophilic Janus granules with an OSA DS that is 68% compared to homogeneously OSA-modified particles. These Janus particles exhibit unique self-assembly behavior into wormlike strings due to their asymmetry. We believe that this unique self-assembly behavior leads to a higher effective dispersed phase volume, which explains why they give a fourfold increase in WHC, a 30% lower CCC, and a viscosity greater by orders of magnitude under certain shear rates. In addition, these particles make gels that are firmer and more shelf stable by orders of magnitude compared to controls.

These unique properties of Janus particles made from starch can be exploited for many potential applications in diverse fields. In the food industry, for example, they can potentially revolutionize the \$12.6 billion global modified starch industry as novel, plant-based super-thickeners or gelling agents that can be used to make lower-calorie food products with lower manufacturing cost-in-use and longer shelf life. Because Janus starch particles build viscosity via a new self-assembly mechanism, as opposed to the traditional, non-Janus starch's classic swelling mechanism, new textures in food products may also be potentially created for the consumer that can give a competitive advantage to food companies that decide to commercially produce or use Janus particles for the first time.

Starch Janus particles may also find use in environmental, cosmetic, and biomedical applications. In the literature on synthetic Janus particles, it is clear that porosity, swellability

(size, shape, softness), and responsiveness to external stimuli like temperature or shear are key parameters that need to be controlled in order to modulate the ability of synthetic Janus particles to adsorb, desorb, pick-up-and-transport, encapsulate, and/or remove cargo (drugs, active ingredients, or toxins). 9,16,52-56 We believe that starch would be a great alternative natural material with the best potential for modulating these parameters in the future. Not only does starch satisfy calls for the use of biocompatible, biodegradable, cheap, widely available, and environmentally friendly materials, it also offers broad versatility in terms of functionalities. We believe that taking advantage of the versatility of a natural biopolymer like starch to synthesize Janus particles may resolve some of the current challenges plaguing the Janus particle field and may point it toward the right direction.

ASSOCIATED CONTENT

Supporting Information

The Supporting Information is available free of charge at https://pubs.acs.org/doi/10.1021/acsami.2c17634.

Validation of wax Pickering method by SEM, ATR-FTIR, DSC, and NMR; SEM image of Janus Polymer amaranth starch in bulk; validation of technique used to measure Janus balance by simulations (PDF)

AUTHOR INFORMATION

Corresponding Author

Alireza Abbaspourrad – Department of Food Science, College of Agriculture and Life Sciences, Cornell University, Ithaca, New York 14853, United States; o orcid.org/0000-0001-5617-9220; Phone: 1 (607) 255-2923; Email: Alireza@ cornell.edu

Authors

Arkaye Kierulf – Department of Food Science, College of Agriculture and Life Sciences, Cornell University, Ithaca, New York 14853, United States; Tate & Lyle Solutions USA LLC, Hoffman Estates, Illinois 60192, United States

Mojtaba Enayati - Department of Food Science, College of Agriculture and Life Sciences, Cornell University, Ithaca, New York 14853, United States

Mohammad Yaghoobi - Department of Food Science, College of Agriculture and Life Sciences, Cornell University, Ithaca, New York 14853, United States

Judith Whaley - Tate & Lyle Solutions USA LLC, Hoffman Estates, Illinois 60192, United States; Present Address: Inverness Insights LLC, 1930 S. Braymore Dr., Inverness, IL 60010, USA

James Smoot – Tate & Lyle Solutions USA LLC, Hoffman Estates, Illinois 60192, United States

Mariana Perez Herrera - Tate & Lyle Solutions USA LLC, Hoffman Estates, Illinois 60192, United States

Complete contact information is available at: https://pubs.acs.org/10.1021/acsami.2c17634

Notes

The authors declare no competing financial interest. CRediT Author Statement; A.K.: conceptualization, formal analysis, investigation, methodology, project administration, writing-original draft, writing-review and editing; M.E.: formal analysis, investigation, methodology, writing-review and editing; M.Y.: formal analysis, investigation, methodology, validation, software; J.W., J.S., and M.P.H.: conceptualization, supervision, writing-review and editing, funding acquisition; A.A.: conceptualization, supervision, methodology, resources, writing-review and editing, funding acquisition.

ACKNOWLEDGMENTS

This work has received funding from Tate & Lyle Solutions USA LLC. The authors would like to acknowledge Veronica Cueva, Weichang Liu, Carmen Moraru, Robin Dando, Uli Wiesner, Michael Selig, Javad Amani Shams Abad, and Mohammad Davachi for their technical guidance. Thanks are also due to David Wise for assembling the glass reaction vessel; Jennifer Burlew and Marti-Jo Russell for conducting protein analysis; and Morteza Azizi, William Guzman, Brenda Werner, Anthony M. Condo Jr., Philip Carubia, and Joseph Dumpler for equipment assistance. Thank you to Erika Louise Mudrak and Brook Luers of the Cornell Statistical Consulting Unit, and to Kelley Donaghy for carefully editing this manuscript. This work also made use of the Cornell Center for Material Research Shared Facilities, which are supported by the National Science Foundation under Award Number DMR-1719875, and the Cornell NMR Facility supported in part by the NSF-MRI grant CHE-1531632.

REFERENCES

- (1) Modified Starch Market. https://www.futuremarketinsights.com/ reports/modified-starch-market (accessed Nov 14, 2022).
- (2) Joyner, H. S.; Wicklund, R. A.; Templeton, C. M.; Howarth, L. G.; Wong, S.-S.; Anvari, M.; Whaley, J. K. Development of Starch Texture Rheological Maps through Empirical Modeling of Starch Swelling Behavior. Food Hydrocolloids 2021, 120, 106920.
- (3) Marschelke, C.; Fery, A.; Synytska, A. Janus Particles: From Concepts to Environmentally Friendly Materials and Sustainable Applications. Colloid Polym. Sci. 2020, 298, 841-865.
- (4) de Gennes, P. G. Soft Matter. Rev. Mod. Phys. 1992, 64, 645-648.
- (5) Loget, G.; Kuhn, A. Bulk Synthesis of Janus Objects and Asymmetric Patchy Particles. J. Mater. Chem. 2012, 22, 15457–15474.
- (6) Liang, F.; Zhang, C.; Yang, Z. Rational Design and Synthesis of Janus Composites. Adv. Mater. 2014, 26, 6944-6949.
- (7) Zhang, J.; Grzybowski, B. A.; Granick, S. Janus Particle Synthesis, Assembly, and Application. Langmuir 2017, 33, 6964-6977.
- (8) Walther, A.; Müller, A. H. E. Janus Particles: Synthesis, Self-Assembly, Physical Properties, and Applications. Chem. Rev. 2013, 113,
- (9) Zhang, L.; Chen, Y.; Li, Z.; Li, L.; Saint-Cricq, P.; Li, C.; Lin, J.; Wang, C.; Su, Z.; Zink, J. I. Tailored Synthesis of Octopus-Type Janus Nanoparticles for Synergistic Actively-Targeted and Chemo-Photothermal Therapy. Angew. Chem., Int. Ed. 2016, 55, 2118-2121.
- (10) Takei, H.; Shimizu, N. Gradient Sensitive Microscopic Probes Prepared by Gold Evaporation and Chemisorption on Latex Spheres. Langmuir 1997, 13, 1865-1868.
- (11) Tanaka, T.; Okayama, M.; Kitayama, Y.; Kagawa, Y.; Okubo, M. Preparation of "Mushroom-like" Janus Particles by Site-Selective Surface-Initiated Atom Transfer Radical Polymerization in Aqueous Dispersed Systems. Langmuir 2010, 26, 7843-7847.
- (12) Kim, S.-H.; Abbaspourrad, A.; Weitz, D. A. Amphiphilic Crescent-Moon-Shaped Microparticles Formed by Selective Adsorption of Colloids. J. Am. Chem. Soc. 2011, 133, 5516-5524.
- (13) Gröschel, A. H.; Walther, A.; Löbling, T. I.; Schmelz, J.; Hanisch, A.; Schmalz, H.; Müller, A. H. E. Facile, Solution-Based Synthesis of Soft, Nanoscale Janus Particles with Tunable Janus Balance. J. Am. Chem. Soc. 2012, 134, 13850-13860.
- (14) Hong, L.; Jiang, S.; Granick, S. Simple Method to Produce Janus Colloidal Particles in Large Quantity. Langmuir 2006, 22, 9495–9499.

- (15) Venkataramani, D.; Tsulaia, A.; Amin, S. Fundamentals and Applications of Particle Stabilized Emulsions in Cosmetic Formulations. *Adv. Colloid Interface Sci.* **2020**, 283, 102234.
- (16) Su, H.; Hurd Price, C.-A.; Jing, L.; Tian, Q.; Liu, J.; Qian, K. Janus Particles: Design, Preparation, and Biomedical Applications. *Materials Today Bio* **2019**, *4*, 100033.
- (17) Li, Q.; Hu, E.; Yu, K.; Lu, M.; Xie, R.; Lu, F.; Lu, B.; Bao, R.; Lan, G. Magnetic Field-Mediated Janus Particles with Sustained Driving Capability for Severe Bleeding Control in Perforating and Inflected Wounds. *Bioact. Mater.* **2021**, *6*, 4625–4639.
- (18) Li, Q.; Hu, E.; Yu, K.; Xie, R.; Lu, F.; Lu, B.; Bao, R.; Zhao, T.; Dai, F.; Lan, G. Self-Propelling Janus Particles for Hemostasis in Perforating and Irregular Wounds with Massive Hemorrhage. *Adv. Funct. Mater.* **2020**, *30*, 2004153.
- (19) Marquis, M.; Renard, D.; Cathala, B. Microfluidic Generation and Selective Degradation of Biopolymer-Based Janus Microbeads. *Biomacromolecules* **2012**, *13*, 1197–1203.
- (20) Zhao, L. B.; Pan, L.; Zhang, K.; Guo, S. S.; Liu, W.; Wang, Y.; Chen, Y.; Zhao, X. Z.; Chan, H. L. W. Generation of Janus Alginate Hydrogel Particles with Magnetic Anisotropy for Cell Encapsulation. *Lab Chip* **2009**, *9*, 2981–2986.
- (21) Kierulf, A.; Azizi, M.; Eskandarloo, H.; Whaley, J.; Liu, W.; Perez-Herrera, M.; You, Z.; Abbaspourrad, A. Starch-Based Janus Particles: Proof-of-Concept Heterogeneous Design via a Spin-Coating Spray Approach. *Food Hydrocolloids* **2019**, *91*, 301–310.
- (22) Li, P.; Kierulf, A.; Wang, J.; Yaghoobi, M.; Whaley, J.; Smoot, J.; Perez Herrera, M.; Abbaspourrad, A. Fabrication of Charged Self-Assembling Patchy Particles Templated with Partially Gelatinized Starch. ACS Appl. Mater. Interfaces 2022, 14, 24955–24963.
- (23) Li, P.; Kierulf, A.; Whaley, J.; Smoot, J.; Herrera, M. P.; Abbaspourrad, A. Modulating Functionality of Starch-Based Patchy Particles by Manipulating Architecture and Environmental Factors. *ACS Appl. Mater. Interfaces* **2022**, *14*, 39497–39506.
- (24) Kierulf, A.; Whaley, J.; Liu, W.; Enayati, M.; Tan, C.; Perez-Herrera, M.; You, Z.; Abbaspourrad, A. Protein Content of Amaranth and Quinoa Starch Plays a Key Role in Their Ability as Pickering Emulsifiers. *Food Chem.* **2020**, *315*, 126246.
- (25) Enayati, M.; Abbaspourrad, A. Facile Preparation of Superhydrophobic and Oleophobic Surfaces via the Combination of Cu(0)-Mediated Reversible-Deactivation Radical Polymerization and Click Chemistry. J. Polym. Sci., Part A: Polym. Chem. 2018, 56, 1684–1694.
- (26) Arshadi, M.; Eskandarloo, H.; Enayati, M.; Godec, M.; Abbaspourrad, A. Highly Water-Dispersible and Antibacterial Magnetic Clay Nanotubes Functionalized with Polyelectrolyte Brushes: High Adsorption Capacity and Selectivity toward Heparin in Batch and Continuous System. *Green Chem.* 2018, 20, 5491–5508.
- (27) Shih, F. F.; Daigle, K. W. Gelatinization and Pasting Properties of Rice Starch Modified with 2-Octen-1-Ylsuccinic Anhydride. *Food/Nahrung* **2003**, *47*, 64–67.
- (28) Farooq, A. M.; Dhital, S.; Li, C.; Zhang, B.; Huang, Q. Effects of Palm Oil on Structural and in Vitro Digestion Properties of Cooked Rice Starches. *Int. J. Biol. Macromol.* **2018**, *107*, 1080–1085.
- (29) Kong, X.; Kasapis, S.; Bertoft, E.; Corke, H. Rheological Properties of Starches from Grain Amaranth and Their Relationship to Starch Structure. *Starch-Stärke* **2010**, *62*, 302–308.
- (30) Singh, N.; Singh Sandhu, K.; Kaur, M. Characterization of Starches Separated from Indian Chickpea (Cicer Arietinum L.) Cultivars. *J. Food Eng.* **2004**, *63*, 441–449.
- (31) Azfaralariff, A.; Fazial, F. F.; Sontanosamy, R. S.; Nazar, M. F.; Lazim, A. M. Food-Grade Particle Stabilized Pickering Emulsion Using Modified Sago (Metroxylon Sagu) Starch Nanocrystal. *J. Food Eng.* **2020**, 280, 109974.
- (32) Saari, H.; Heravifar, K.; Rayner, M.; Wahlgren, M.; Sjöö, M. Preparation and Characterization of Starch Particles for Use in Pickering Emulsions. *Cereal Chem.* **2016**, 93, 116–124.
- (33) Li, C.; Li, Y.; Sun, P.; Yang, C. Pickering Emulsions Stabilized by Native Starch Granules. *Colloids Surf., A* **2013**, 431, 142–149.
- (34) Zhao, S.; Tian, G.; Zhao, C.; Lu, C.; Bao, Y.; Liu, X.; Zheng, J. Emulsifying Stability Properties of Octenyl Succinic Anhydride (OSA)

- Modified Waxy Starches with Different Molecular Structures. *Food Hydrocolloids* **2018**, *85*, 248–256.
- (35) Official Methods of Analysis, 2019, 21st ed.; AOAC International. https://www.aoac.org/official-methods-of-analysis-21st-edition-2019/ (accessed Nov 14, 2022).
- (36) Hui, R.; Qi-he, C.; Ming-liang, F.; Qiong, X.; Guo-qing, H. Preparation and Properties of Octenyl Succinic Anhydride Modified Potato Starch. *Food Chem.* **2009**, *114*, 81–86.
- (37) Ye, F.; Miao, M.; Huang, C.; Lu, K.; Jiang, B.; Zhang, T. Elucidation of Substituted Ester Group Position in Octenylsuccinic Anhydride Modified Sugary Maize Soluble Starch. *J. Agric. Food Chem.* **2014**, *62*, 11696–11705.
- (38) Miao, M.; Li, R.; Jiang, B.; Cui, S. W.; Zhang, T.; Jin, Z. Structure and Physicochemical Properties of Octenyl Succinic Esters of Sugary Maize Soluble Starch and Waxy Maize Starch. *Food Chem.* **2014**, *151*, 154–160.
- (39) Whitney, K.; Reuhs, B. L.; Ovando Martinez, M.; Simsek, S. Analysis of Octenylsuccinate Rice and Tapioca Starches: Distribution of Octenylsuccinic Anhydride Groups in Starch Granules. *Food Chem.* **2016**, *211*, 608–615.
- (40) Xia, X.; Li, G.; Liao, F.; Zhang, F.; Zheng, J.; Kan, J. Granular Structure and Physicochemical Properties of Starches from Amaranth Grain. *Int. J. Food Prop.* **2015**, *18*, 1029–1037.
- (41) Bhosale, R.; Singhal, R. Effect of Octenylsuccinylation on Physicochemical and Functional Properties of Waxy Maize and Amaranth Starches. *Carbohydr. Polym.* **2007**, *68*, 447–456.
- (42) Li, Z.-W.; Lu, Z.-Y.; Sun, Z.-Y.; An, L.-J. Model, Self-Assembly Structures, and Phase Diagram of Soft Janus Particles. *Soft Matter* **2012**, *8*, 6693–6697.
- (43) Chen, Q.; Whitmer, J. K.; Jiang, S.; Bae, S. C.; Luijten, E.; Granick, S. Supracolloidal Reaction Kinetics of Janus Spheres. *Science* **2011**, 331, 199–202.
- (44) Elhardallou, S. B.; Walker, A. F. The Water-Holding Capacity of Three Starchy Legumes in the Raw, Cooked and Fibre-Rich Fraction Forms. *Plant Foods Hum. Nutr.* **1993**, *44*, 171–179.
- (45) McClements, D. J.Food Emulsions: Principles, Practices, and Techniques, 3rd ed.; CRC Press: Boca Raton, 2015; pp 294-295.
- (46) Chanamai, R.; McClements, D. J. Dependence of Creaming and Rheology of Monodisperse Oil-in-Water Emulsions on Droplet Size and Concentration. *Colloids Surf., A* **2000**, *172*, 79–86.
- (47) Timgren, A.; Rayner, M.; Dejmek, P.; Marku, D.; Sjöö, M. Emulsion Stabilizing Capacity of Intact Starch Granules Modified by Heat Treatment or Octenyl Succinic Anhydride. *Food Sci. Nutr.* **2013**, *1*, 157–171.
- (48) Yu, Z.-Y.; Jiang, S.-W.; Zheng, Z.; Cao, X.-M.; Hou, Z.-G.; Xu, J.-J.; Wang, H.-L.; Jiang, S.-T.; Pan, L.-J. Preparation and Properties of OSA-Modified Taro Starches and Their Application for Stabilizing Pickering Emulsions. *Int. J. Biol. Macromol.* **2019**, *137*, 277–285.
- (49) Liu, W.; Li, Y.; Goff, H. D.; Nsor-Atindana, J.; Ma, J.; Zhong, F. Interfacial Activity and Self-Assembly Behavior of Dissolved and Granular Octenyl Succinate Anhydride Starches. *Langmuir* **2019**, *35*, 4702–4709.
- (50) Aveyard, R. Can Janus Particles Give Thermodynamically Stable Pickering Emulsions? *Soft Matter* **2012**, *8*, 5233–5240.
- (51) Kumar, A.; Park, B. J.; Tu, F.; Lee, D. Amphiphilic Janus Particles at Fluid Interfaces. *Soft Matter* **2013**, *9*, 6604–6617.
- (52) Safaie, N.; Ferrier, R. C. Janus Nanoparticle Synthesis: Overview, Recent Developments, and Applications. *J. Appl. Phys.* **2020**, *127*, 170902.
- (53) Li, X.; Zhou, L.; Wei, Y.; El-Toni, A. M.; Zhang, F.; Zhao, D. Anisotropic Growth-Induced Synthesis of Dual-Compartment Janus Mesoporous Silica Nanoparticles for Bimodal Triggered Drugs Delivery. J. Am. Chem. Soc. 2014, 136, 15086–15092.
- (54) Orozco, J.; Mercante, L. A.; Pol, R.; Merkoçi, A. Graphene-Based Janus Micromotors for the Dynamic Removal of Pollutants. *J. Mater. Chem. A* **2016**, *4*, 3371–3378.
- (55) Lu, A. X.; Liu, Y.; Oh, H.; Gargava, A.; Kendall, E.; Nie, Z.; DeVoe, D. L.; Raghavan, S. R. Catalytic Propulsion and Magnetic Steering of Soft, Patchy Microcapsules: Ability to Pick-Up and Drop-

Off Microscale Cargo. ACS Appl. Mater. Interfaces 2016, 8, 15676-

(56) Li, W.; Liu, Y.; Brett, G.; Gunton, J. D. Encapsulation by Janus Spheroids. Soft Matter 2012, 8, 6027-6032.

Recommended by ACS

Structure-Based Design of Dual Bactericidal and Bacteria-**Releasing Nanosurfaces**

Daniel Salatto, Tadanori Koga, et al.

JANUARY 04, 2023

ACS APPLIED MATERIALS & INTERFACES

READ

In Situ Formation of Soft-Rigid Hybrid Fibers Decorated by Sparse Lamellae of PLLA: Achieving Ductile and Heat-**Resistant Materials with High Strength**

Pengfei Liu, Jianhui Qiu, et al.

JANUARY 04, 2023

MACROMOLECULES

READ 🗹

Interplay of Polymer Structure, Solvent Ordering, and **Charge Fluctuations in Polyelectrolyte Solution Thermodynamics**

Michael Beckinghausen and Andrew J. Spakowitz

DECEMBER 27, 2022

MACROMOLECULES

READ 🗹

Combined Mixing and Dynamical Origins of T_{e} Alterations **Near Polymer-Polymer Interfaces**

Asieh Ghanekarade and David S. Simmons

DECEMBER 30, 2022

MACROMOLECULES

READ 🗹

Get More Suggestions >